Environmental Pollution 335 (2023) 122283

Contents lists available at ScienceDirect

Environmental Pollution

journal homepage: www.elsevier.com/locate/envpol

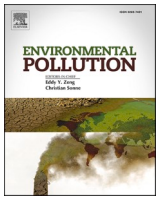

Contributions of non-tailpipe emissions to near-road $PM_{2.5}$ and PM_{10}: A chemical mass balance study☆

L.-W. Antony Chen [a,b,*], Xiaoliang Wang [b], Brenda Lopez [c], Guoyuan Wu [c], Steven Sai Hang Ho [b], Judith C. Chow [b], John G. Watson [b], Qi Yao [d], Seungju Yoon [d], Heejung Jung [c]

[a] Department of Environmental and Occupational Health, School of Public Health, University of Nevada, Las Vegas, 4505 S. Maryland Pkwy, Las Vegas, NV, 89154, USA
[b] Division of Atmospheric Sciences, Desert Research Institute, 2215 Raggio Pkwy, Reno, NV, 89512, USA
[c] Department of Mechanical Engineering and Center for Environmental Research and Technology (CE-CERT), University of California-Riverside, 1084 Columbia Ave, Riverside, CA, 92507, USA
[d] Research Division, California Air Resources Board, 1001 I St, Sacramento, CA, 95814, USA

ARTICLE INFO

Keywords:
Brake wear
Tire wear
Source profile
Source apportionment
Hybrid environmental receptor model (HERM)

ABSTRACT

As the importance of non-tailpipe particles (NTP) over tailpipe emissions from urban traffic has been increasing, there is a need to evaluate NTP contributions to ambient particulate matter (PM) using representative source profiles. The Brake and Tire Wear Study conducted in Los Angeles, California in the winter of 2020 collected 64 $PM_{2.5}$ and 64 PM_{10} samples from 32 pairs of downwind-upwind measurements at two near-road locations (I-5 in Anaheim and I-710 in Long Beach). These samples were characterized for inorganic and organic markers and, along with locally-developed brake wear, tire wear, and road dust source profiles, subject to source apportionment using the effective-variance chemical mass balance (EV-CMB) model. Model results highlighted the dominance of resuspended dust in both $PM_{2.5}$ (23–33%) and PM_{10} (32–53%). Brake and tire wear contributed more to $PM_{2.5}$ than tailpipe exhausts (diesel + gasoline) for I-5 (29–30% vs. 19–21%) while they were comparable for I-710 (15–17% vs. 15–19%). For PM_{10}, the brake and tire wear contributions were 2–3 times the exhaust contributions. Different fleet compositions on and near I-5 and I-710 appeared to influence the relative importance of NTP and exhaust sources. The downwind-upwind differences in source contributions were often insignificant, consistent with small and/or nearly equal impacts of adjacent highway traffic emissions on the downwind and upwind sites. The utility of sole markers, such as barium and zinc, to predict brake and tire wear abundances in ambient PM is evaluated.

1. Introduction

Elevated pollutant concentrations in near-road environments have been a concern for health effects and disparity (Clark et al., 2017; Rowangould, 2013). Epidemiologic studies have linked vehicular emissions to health burdens, such as increased asthma attacks, cardiac and pulmonary diseases, impaired lung function, and low birth weights (Brandt et al., 2014; Brugge et al., 2007; Ghosh et al., 2016; HEI, 2022). Regulatory efforts by air quality agencies globally have resulted in decreasing tailpipe emissions over the years, but non-tailpipe emissions, such as brake and tire wear particles, are not affected by these efforts (Harrison et al., 2021). Battery electric vehicles, which are gaining market penetration, achieve zero tailpipe emissions but potentially generate higher brake and tire wear emissions than conventional vehicles due to their heavier weights (Beddows and Harrison, 2021; Timmers and Achten, 2016). Thus, the importance of non-tailpipe particles (NTP) to ambient particulate matter (PM) increases (Amato et al., 2014; Denier van der Gon et al., 2013). The statewide California Air Resources Board's emission inventory (California Air Resources Board, 2021) estimates that brake and tire wear have exceeded tailpipe in $PM_{2.5}$ (particles with aerodynamic diameters $\leq$2.5 μm) emissions since 2020. This is of concern since brake and tire particles have higher metal contents,

☆ This paper has been recommended for acceptance by Admir Créso Targino.

* Corresponding author. Department of Environmental and Occupational Health, School of Public Health, University of Nevada, Las Vegas, 4505 S. Maryland Pkwy, Las Vegas, NV, 89154, USA.
E-mail address: antony.chen@unlv.edu (L.-W.A. Chen).

https://doi.org/10.1016/j.envpol.2023.122283
Received 26 March 2023; Received in revised form 3 July 2023; Accepted 27 July 2023
Available online 28 July 2023

possibly resulting in higher toxicity and adverse health outcomes for traffic-impacted communities.

Brake wear resulting from abrasion of brake pads and rotors contains trace metals such as iron (Fe), manganese (Mn), copper (Cu), titanium (Ti), zinc (Zn), antimony (Sb), and barium (Ba) (Pant and Harrison, 2013). Rubber polymers, their derivatives, and carbon black dominate tire wear, while Zn and benzothiazoles are often used as tire wear markers (Klöckner et al., 2019; Pant and Harrison, 2013; Wik and Dave, 2009). Zinc oxide, organozinc compounds, and benzothiazoles are added to tire tread during the vulcanization process. Tire wear particles can contain polycyclic aromatic hydrocarbons (PAHs) and n-alkanes, likely created through volatilization during contact of the tire tread with road surfaces and subsequent condensation into the particle phase (Aatmeeyata and Sharma, 2010; Baensch-Baltruschat et al., 2020). NTP may also include resuspended road dust/wear which is rich in mineral elements such as silicon (Si), aluminum (Al), and calcium (Ca). Compared to tailpipe exhaust particles that are primarily submicron in size, NTP markers are found in both fine- and coarse-mode particles (Harrison et al., 2012; Lin et al., 2015; Lough et al., 2005).

Quantifying NTP contributions to fine- ($PM_{2.5}$) and coarse-mode (PM_{10} and $PM_{10\text{-}2.5}$: particles with aerodynamic diameters $\leq$10 μm and between 2.5 and 10 μm, respectively) remains a challenge. Harrison et al. (2012) estimated brake wear, tire wear, and road dust contributions to size-segregated PM using Ba, Zn, and Si as markers and assuming brake-wear/Ba, tire-wear/Zn, and dust/Si mass ratios of 91, 50, and 3.6, respectively. This approach doesn't take into account that Zn can result from both brake and tire wear whereas there are possibly other sources of Ba, Zn, and/or Si in the study area. Factor analysis models such as principle component analysis (PCA) and positive matrix factorization (PMF) sought to discern NTP factor(s) in a multivariate dataset that contains major markers (Amato et al., 2011; Fabretti et al., 2009; Jalali Farahani et al., 2022; Lawrence et al., 2013). However, temporal correlations among NTP and tailpipe emissions often cause them to mix into single factor(s), thus biasing the source apportionment (Chen et al., 2010a). Despite of the uncertainty, NTP were found to rival exhaust particles in their abundances, particularly in urban PM_{10} and $PM_{10\text{-}2.5}$ (Harrison et al., 2021).

With a high population density and heavy traffic, elevated air pollution levels in the Los Angeles metropolitan region of southern California have been well documented. Hasheminassab et al. (2014a,b) attributed long-term $PM_{2.5}$ concentrations to vehicular emissions, secondary nitrate, secondary sulfate, soil, aged sea salt, fresh sea salt, and biomass burning, with vehicular emissions accounting for ~20% of $PM_{2.5}$ for the period of 2002–2013. NTP were not resolved in that study, though they were likely incorporated into vehicular emissions and/or soil factors. Habre et al. (2021) identified similar sources across Los Angeles in 2008–2009, but attributed 11% and 21% of $PM_{2.5}$ to NTP (brake + tire) and exhaust particles, respectively, and 18% of $PM_{10\text{-}2.5}$ to NTP (brake + tire). A more recent study (Jalali Farahani et al., 2022) near Los Angeles highways found similar contributions of NTP (brake + tire) and exhaust particles to PM_{10}, at 16% and 26%, respectively.

To further understand real-world non-tailpipe emissions and contributions to exposure, $PM_{2.5}$ and PM_{10} were sampled downwind and upwind of two major highways in Los Angeles during the winter of 2020 and subsequently analyzed for elemental and organic compositions (Lopez et al., 2023; Wang et al., 2023). These data were used in the effective variance-chemical mass balance (EV-CMB) model with explicit brake and tire wear source profiles to obtain source contribution estimates. The results add to literature and emission inventories that highlight the importance of NTP in urban air pollution while informing regulatory strategies needed to attain ambient air quality standards.

2. Materials and methods

2.1. $PM_{2.5}$ and PM_{10} data

Time-integrated $PM_{2.5}$ and PM_{10} samples were collected near highway I-5 in Anaheim and near highway I-710 in Long Beach (Fig. 1) over a two-week period. I-5 and I-710 are paved with concrete and asphalt, respectively. On-site traffic counts during the tests indicated ~95% light-duty vehicles (LDV) and 5% heavy-duty vehicles (HDV) on I-5, representative of a typical southern California highway fleet, and ~90% LDV and 10% HDV on I-710, consistent with goods movement to and from the Ports of Long Beach and Los Angeles (Wang et al., 2023).

Sampling occurred simultaneously on both sides of each highway and as close as logistically possible to the highway, i.e., <30 m from the nearest traffic lane except for the upwind I-710 site (~100 m from the nearest lane). Samples were acquired using DRI medium-volume sequential samplers (Chow et al., 1993) each day from 0600 to 1000 local standard time (LST) to represent morning rush hours, 1000 to 1400 LST for midday traffic, and 1400 to 1800 LST for evening rush hours. The sampling flow rate was 37.7 L/min. A total of 64 $PM_{2.5}$ and 64 PM_{10} samples from 32 pairs (18 at Anaheim and 14 at Long Beach) of downwind/upwind measurements were available for subsequent chemical analysis.

Each sample set was characterized for $PM_{2.5}$ or PM_{10} mass, 51 elements, water soluble cations and anions such as sodium (Na^+), potassium (K^+), sulfate (SO_4^{2-}) and nitrate (NO_3^-), as well as organic carbon (OC), elemental carbon (EC), and thermal carbon fractions (OC1-OC4, OP, EC1-EC3). Non-polar organic speciation included PAHs, alkanes, alkenes, hopanes, steranes, and phthalates that are common combustion markers (Ambade et al., 2023; Fadel et al., 2021; Kumar et al., 2020). Tire markers such as benzothiazole and its derivatives, as well as thermal decomposition fragments of rubber (styrene, butadiene, etc.), were also analyzed. Wang et al. (2023) documents the analytical methods and quality assurance/control in detail.

2.2. Receptor modeling

The EV-CMB- model (Watson et al., 1984) was employed to quantify source-specific contributions to $PM_{2.5}$ and PM_{10} by solving:

$$C_{it} = \sum_{j=1}^{J} F_{ij} S_{jt} \tag{1}$$

where C_{it} is the measured concentration of species i in $PM_{2.5}$ or PM_{10} at time t, F_{ij} is the fraction of species i in source profile j, and S_{jt} is the contribution of source j at time t. To achieve valid results, source profiles should be representative of emissions typical of the times and locations of the receptor samples. The source contribution estimates (SCEs), S_{jt}, were calculated by the Hybrid Environmental Receptor Model (HERM) software using an iterative method (Chen and Cao, 2018; Chen et al., 2021) to minimize the chi-square:

$$\chi_t^2 = \frac{1}{I-J} \sum_{i=1}^{I} \frac{\left(C_{it} - \sum_{j=1}^{J} F_{ij} S_{jt}\right)^2}{EV_{it}} \tag{2}$$

where I and J indicate number of species and sources, respectively, in the model and EV_{it} is the effective variance due to uncertainties in both measured ambient concentrations ($\sigma_{C_{it}}$) and source profiles ($\sigma_{F_{ij}}$):

$$EV_{it} = \sigma_{C_{it}}^2 + \sum_{j=1}^{J} \sigma_{F_{ij}}^2 S_{jt}^2 \tag{3}$$

As recommended by Watson (2004) and Chen et al. (2010b, 2012), sensitivity tests should be performed on selected sample(s) to evaluate how different combinations of source profiles and species affect SCEs

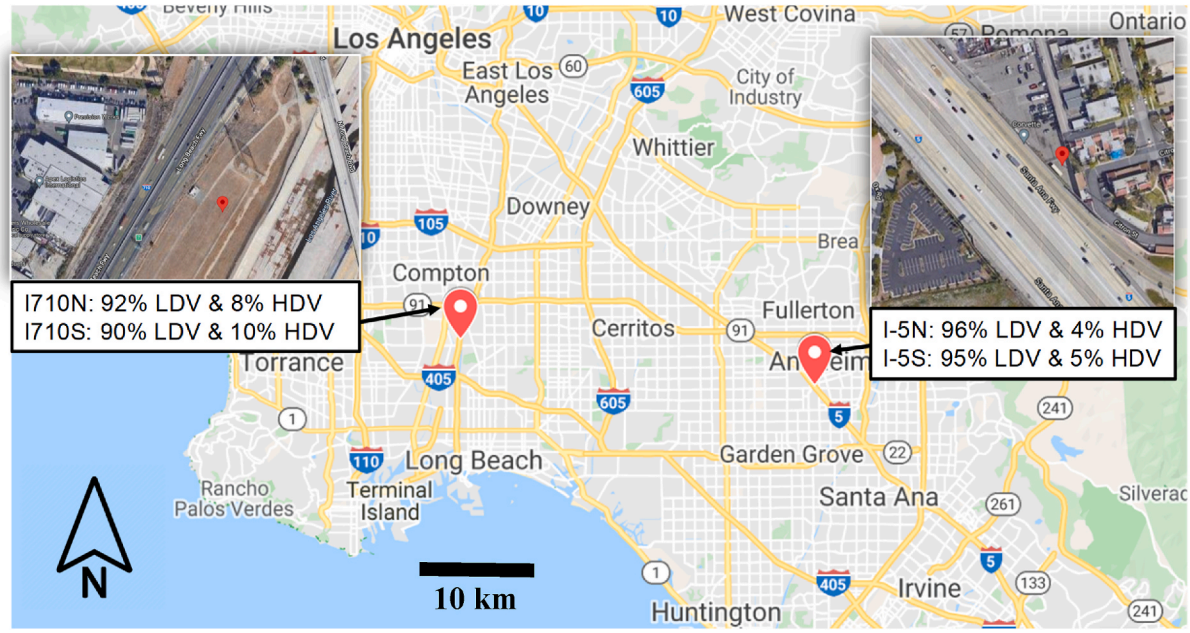

Fig. 1. Near I-5 and I-710 sampling sites in Los Angeles, California during the winter 2020 campaign. Average HDV and LDV fractions for the northbound and southbound traffic are indicated. This map derives from Google Maps.

and model fitting performance. An acceptable solution requires percent mass (%mass) explained between 80 and 120, correlation (r^2) > 0.8, and chi-square (χ^2) < 4. In addition, the modified pseudo-inverse normalized (MPIN) matrix indicates the most influential species (e.g., with MPIN values > 0.4) for each source type. Five to ten different source combinations are typically attempted until the best solution, in terms of EV-CMB performance measures and the MPIN criteria, are attained. Uncertainties of the final SCEs (i.e., $\sigma_{S_{jt}}$) are estimated by

$$\sigma_{S_{jt}}{}^2 = d\left(F'\left(dEV_{ii,t}\right)^{-1}F\right)_{jj}^{-1} \times \chi_t{}^2 \quad (4)$$

where d indicates the diagonal matrix operation. The uncertainties take into account the measurement precision, profile variability, and model goodness of fit.

2.3. Source profiles

Source profiles assembled for southern California are listed in supplemental Table S1. As part of this study, four dust samples were collected near the monitoring sites to develop local fine ($PM_{2.5}$) and coarse (PM_{10}) dust profiles (Wang et al., 2023). These profiles are best characterized as "Resuspended Dust", as they can contain road and windblown dust, local soil, as well as other geological material. To examine the mass closure, reconstructed mass (RM) was calculated for these profiles following Malm and Day (2000): RM = 4.125 × [Sulfur (S)] + 1.29 × [NO_3^-] + 1.4 × [OC] + [EC] + [Crustal Material] + [Trace Elements], where Crustal Material equals 2.2 × [Al] + 2.49 × [Si] + 1.63 × [Ca] + 1.94 × [Ti] + 2.42 × [Fe] and Trace Elements include all elements except S, Al, Si, Ca, Ti, and Fe. Crustal Material ranged 20–34% of the fine mass and 41–62% of the coarse mass. In general, fine dust exhibited a lower mass closure in terms of the RM/PM mass ratio (47–61%) than coarse dust (60–92%). The best mass closure was found for the PM_{10} dust collected downwind of I-5. Four composite dust profiles were further calculated from the individual profiles (Table S1) following Chow et al. (2003).

Brake dust samples were collected from laboratory experiments and analyzed for chemical composition as part of the California Regional Particulate Air Quality Study (CRPAQS, see Fitz et al. (2004)). Mass fractions of Fe, Ba, Mn, and Cu, known brake wear markers, were found to be 20–66%, 3–13%. 0.2–0.6%, and 0.04–0.08%, respectively, in the brake $PM_{2.5}$. A recent inertial dynamometer study (Agudelo et al., 2020) examined brake wear PM_{10} compositions from six light-duty vehicles using a test cycle typical of that followed in California. The results were composited into four brake source profiles reflecting different brake pad materials and positions (Table S1). The mass fractions of Fe, Ba, Mn, and Cu in these profiles are 11–47%, 1–11%, 0.1–0.7%, and 0.04–4.9%, respectively, with two brake profiles showing much higher Cu contents (4.9% and 1.7%) than observed in CRPAQS.

CRPAQS also reported two tire wear profiles, which are dominated by OC and EC and contain elevated levels of Fe (18–22%), Zn (2–3%), Si (3%), Al (2–3%), Ca (2%), and Cu (1–2%). Such levels of crustal elements, especially Fe, in tire wear are not expected. As part of this study, tire wear particles without size segregation were collected from a dynamometer test of Michelin and Cooper tires (Wang et al., 2023). This produced two tire wear profiles that are also dominated by OC and EC (>75%). The two tire profiles differ the most for the Si abundance (0.6% for Michelin versus 6% for Cooper), while the Fe, Zn, Al, Ca, and Cu fractions range 0.1–0.2%, 0.5–1%, 0.04–0.2%, 0.07–0.1%, and 0.003–0.004%, respectively. Zn appears to be a consistent marker for tire wear, whereas other species abundances are more variable compared to the CRPAQS profiles.

Since tailpipe exhaust profiles were not developed specifically for this study, those acquired for the National Renewable Energy Laboratory Gas/Diesel Split Study (Fujita et al., 2007a, 2007b) were used. The Gas/Diesel Split Study measured $PM_{2.5}$ emissions from 59 light-duty (including 57 gasoline- and 2 diesel-fueled vehicles) and 30 medium- and heavy-duty diesel-fueled vehicles. It was conducted at a grocery distribution center in Riverside, CA, during the summer and winter of 2001 using a constant volume sampling system. Profiles developed from that study include low emitters, high emitters, and black carbon (BC) emitters for gasoline vehicles under cold and warm start conditions, as well as medium-duty and heavy-duty diesel vehicles under city and highway driving cycles. These profiles are more recent and contain full organic speciation (except for alkanes). Its gasoline and diesel composite profiles (GAS and DIESEL) have been successfully applied to $PM_{2.5}$ source apportionment for California and Nevada fleets (Chen et al., 2012; Chow et al., 2007).

In addition to NTP and engine exhaust profiles, secondary nitrate and

sulfate were represented by pure ammonium nitrate (NH_4NO_3) and ammonia sulfate ($[NH_4]_2SO_4$) profiles, respectively, in the EV-CMB modeling. Previous studies show that sea salt, biomass burning, industrial emissions, and secondary organic aerosol (SOA) may also contribute to Los Angeles PM (Habre et al., 2021; Hasheminassab et al., 2014; Jalali Farahani et al., 2022). Given the highway-dominated sampling locations, absence of wildfire smoke, and low atmospheric oxidation capacity during the sampling period, these sources were not considered in the EV-CMB analysis. The usual chemical markers for biomass burning (K and K^+) and sea salt (Na^+ and Cl^-) were excluded from the fitting species. Important NTP and engine exhaust markers were among the fitting species: 1) Al, Si, Ti, and Ca for road dust; 2) Fe, Ba, Mn, Cu, and Sb for brake wear; 3) Zn, OC, and phthalates for tire wear; 4) EC and hopanes for diesel engine exhaust; 5) PAHs such as indeno[1,2,3,cd]pyrene, benzo[g,h,i]perylene, and coronene for gasoline engine exhaust; and 6) sulfur (S) and NO_3^- for secondary inorganics. OC fractions (OC1-OC4) were also included. Although both motor vehicle exhaust and tire wear are dominated by organic matter, they can differ significantly in their OC fractions.

3. Results and discussion

3.1. Sensitivity tests

Sensitivity tests evaluate the performance of different source profile combinations in terms of r^2, χ^2, and %mass. To create a sample that is suitable for the sensitivity test, upwind concentrations at the I-5 site were subtracted from the corresponding downwind concentrations so that the differences could be fully attributed to traffic-related emissions including: 1) brake wear, 2) tire wear, 3) road dust, and 4) tailpipe exhausts. Since wind directions varied from time to time, here the downwind and upwind samples for each specific period were designated as the one with higher and lower reconstructed mass, respectively. Sometimes the differences between downwind and upwind concentrations were insignificant (i.e., within the measurement uncertainties). To improve the signal-to-noise ratio, the 18 downwind-upwind-difference compositions were further averaged to produce the chemical profile shown in Fig. 2(a) for the sensitivity tests.

Sensitivity test results are shown in Tables S2 and S3. Inclusion of any single brake profile led to poor fits (low r^2 and high χ^2) for both $PM_{2.5}$ and PM_{10}, likely due to the wide range of brake PM chemical

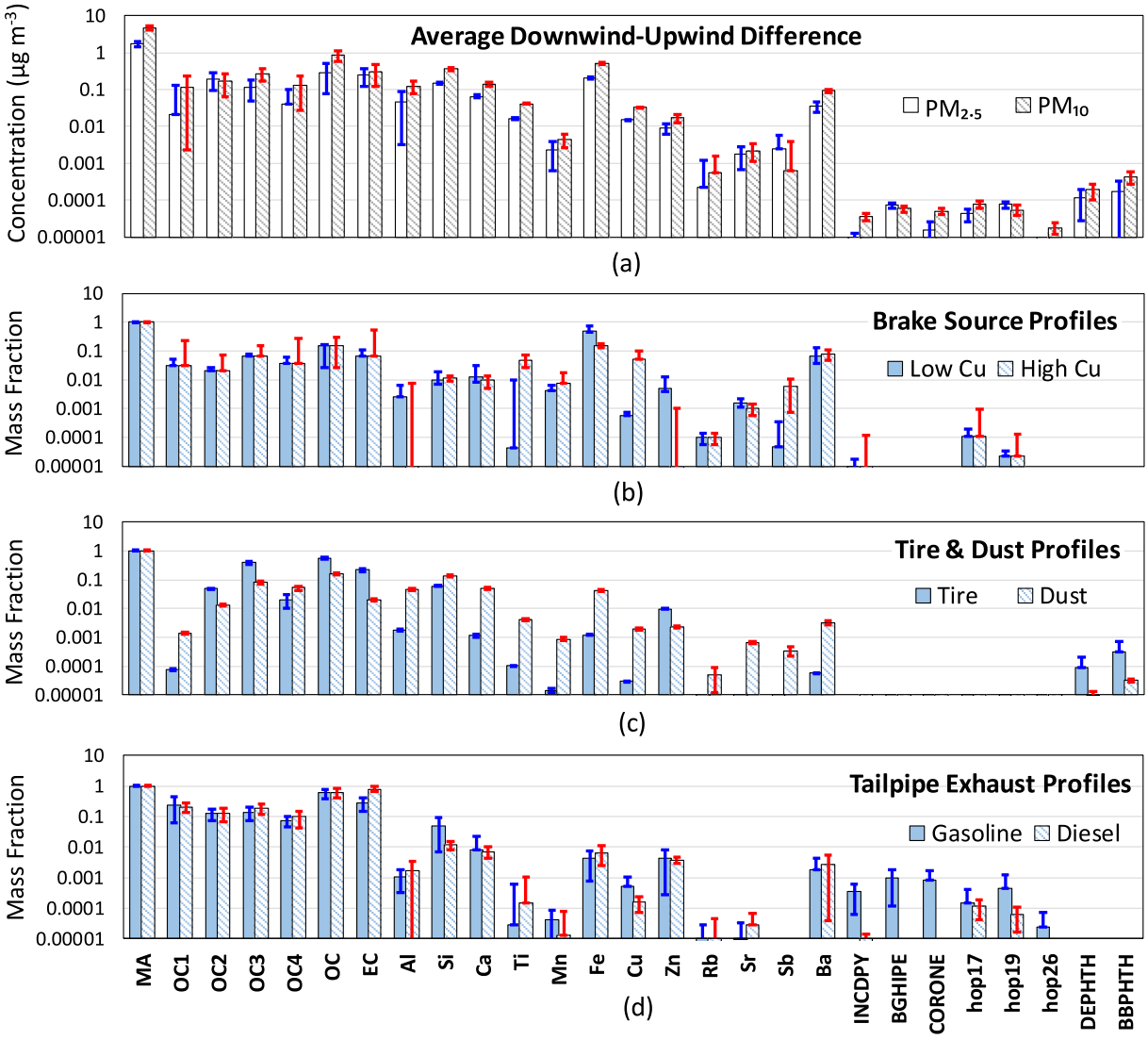

Fig. 2. Chemical compositions of: (a) ambient samples and (b)–(d) optimal source profiles derived from sensitivity tests. The ambient samples were derived from the downwind-upwind differences of I-5 near-road measurements. MA: mass; INCDYP: indeno[1,2,3,cd]pyrene; BGHIPE: benzo[g,h,i]perylene; CORONE: coronene; hop17: αβ-norhopane (C29αβ-hopane); hop19: αβ-hopane (C30αβ -hopane); hop26: 22 S-trishomohopane (C33); DEPHTH: diethyl phthalate; and BBPHTH: butyl benzyl phthalate.

compositions within the fleet. A combination of two brake profiles, BRAKE_C (low Cu) and BRAKE_D (high Cu), achieved the optimal fitting performance. These two brake profiles differ mostly by their Cu and Ti abundances relative to Fe, with ratios of 1.2×10^{-3} and 8.8×10^{-5} in BRAKE_C, respectively, compared with 0.33 and 0.34 in BRAKE_D.

For $PM_{2.5}$, using dust profiles representative of local fine dust particles all produced %mass well above 120 while using dust profiles representative of coarse dust particles (i.e., PM_{10}) produced more reasonable %mass. This is consistent with the lower mass closure in the fine dust profiles (47–61%). Overall, a PM_{10} dust profile originating from I-5 downwind (CCDust, with a mass closure of 92%) led to the best fitting performance. Alternating different tire, gasoline exhaust, and/or diesel exhaust profiles resulted in minor changes to SCEs. Fig. 2(b)–(d) show the final selected combination, which contains an individual tire profile (COTIRE), a composite gasoline exhaust profile (GAS), and a composite diesel exhaust profile (DIESEL), in addition to BRAKE_C, BRAKE_D, and CCDust. This combination led to r^2, χ^2, and %mass of 0.94, 0.78, and 102, respectively, for $PM_{2.5}$ (Table S2), while it also produced a good fit for PM_{10} with a lower %mass at 84 (Table S3). Although a better %mass in PM_{10} could be achieved by replacing CCDust with a composite dust profile (MCDust), this was at the expense of r^2. The same source profile combination was eventually applied to $PM_{2.5}$ and PM_{10} samples for consistency.

The EV-CMB MPIN values are normalized such that they range from −1 to 1. Species with MPIN values of 0.4–1 are considered influential species for a specific source. The MPIN matrices for the selected model inputs (Table S4-S5) indicate that the most important BRAKE_C marker is Fe, followed by Ba while the BRAKE_D contribution is influenced most by Ti and Cu. For tire wear, the most influential markers are OC3 and Zn, followed by OC and diethyl phthalate (DEPHTH). As expected, the CCDust SCE is influenced by Si and Ca. Three PAH species, indeno[1,2,3,cd]pyrene (INCDPY), benzo[g,h,i]perylene (BGHIPE), and coronene (CORONE) are highlighted for gasoline exhaust while EC and C29αβ-hopane (hop17) mark diesel exhaust. These findings are consistent with known source characteristics.

3.2. Source contribution estimates

Using the EV-CMB model established by the sensitivity tests, along with AMNIT and AMSUL to account for secondary nitrate and sulfate, respectively, in the background air, SCEs for $PM_{2.5}$ and PM_{10} at the I-5 downwind and upwind sites were determined (Figure S1). Performance measures attained the guideline of $r^2 > 0.8$ and $\chi^2 < 4$ for 29 of the 36 $PM_{2.5}$ samples and all of the 36 PM_{10} samples. Due to the exclusion of sources such as sea salt, biomass burning, and SOA, %mass tended to be < 100. The source apportionment for the I-710 samples (Figure S2) used the same source combination as for I-5, except that CCDust was replaced with AQDust from I-710 resuspended dust. Satisfactory performance measures ($r^2 > 0.8$ and $\chi^2 < 4$) were achieved for all of the 28 $PM_{2.5}$ samples and 20 of the 28 PM_{10} samples near I-710. Lower performance measure values for some samples led to higher SCE uncertainties.

Table 1 compares mean SCEs for I-5 and I-710. These contributions resulted not only from traffic on the adjacent highways but also from emissions incorporated into the urban background. Resuspended dust was found to dominate and contribute significantly more to PM_{10} than to $PM_{2.5}$ ($p < 0.05$). The contributions of brake wear and tire wear were also higher in PM_{10}, but the differences between $PM_{2.5}$ and PM_{10} were not significant due to large standard errors in the SCEs. Brake_C (low copper) exceeded Brake_D (high copper) for I-5, but the reverse was true for I-710, likely reflecting different fleet mixes. The downwind-upwind differences of NTP (brake wear, tire wear, and road dust) contributions were small, although the downwind sites generally observed higher values, especially at I-5. As noted, the nominal downwind sites (Fig. 1) were not always downwind due to wind directions changing throughout the day (Lopez et al., 2023; Wang et al., 2023).

For gasoline and diesel exhausts, similar contributions were found between $PM_{2.5}$ and PM_{10} ($p > 0.05$), consistent with the dominance of fine particles in tailpipe emissions. The downwind-upwind differences were also insignificant. Diesel contributions appeared higher at I-710 (1.75–1.92 μg m^{-3}) than at I-5 (1.13–1.48 μg m^{-3}) while the gasoline contributions to $PM_{2.5}$ were higher at I-5 (0.61–0.77 μg m^{-3}) than at I-710 (0.26–0.31 μg m^{-3}). The higher fraction of HDV, mostly diesel-fueled, on I-710 did not lead to more brake (Brake_C + Brake_D) and tire wear contributions to $PM_{2.5}$ and PM_{10} (Table 1). More frequent congestion and a generally slower traffic speed near the I-710 segment (Wang et al., 2023) might explain the observation.

Secondary ammonium nitrate was more abundant at I-710 than at I-5, consistent with higher NO_x emissions from HDV, while secondary ammonium sulfate appeared to be uniform across the study area. The high concentrations of nitrate and sulfate in PM_{10} (Table 1) are attributed to displacement of chloride in coarse sea salt by NO_3^- and SO_4^{2-} and the reactions of NO_3^- and SO_4^{2-} with mineral dust (Wang et al., 2023).

3.3. NTP vs. exhaust fractions

For the I-5 sites, resuspended dust accounted for 26–33% and 50–53% of $PM_{2.5}$ and PM_{10} mass, respectively (Fig. 3). The dust fractions were higher than those often found at Los Angeles urban sites (e.g., Hasheminassab et al., 2014), likely reflecting the near-road microenvironment. For $PM_{2.5}$, the brake and tire fractions (brake + tire = ~30%) exceeded the exhaust fractions (diesel + gasoline = ~20%). The unaccounted mass was minor (2–7%). For PM_{10}, the brake and tire fractions (brake + tire) were ~15%, more than twice the exhaust fractions (diesel + gasoline) of ~6%. This is consistent with the higher amounts of NTP in

Table 1
Mean and standard error of source contribution estimates (SCEs in μg m^{-3}) for $PM_{2.5}$ and PM_{10} measured at I-5 and I-710 downwind/upwind sites.

	Anaheim (I-5)				Long Beach (I-710)			
	Downwind		Upwind		Downwind		Upwind	
	$PM_{2.5}$	PM_{10}	$PM_{2.5}$	PM_{10}	$PM_{2.5}$	PM_{10}	$PM_{2.5}$	PM_{10}
# of Data	18	18	18	18	14	14	14	14
Total Mass	10.9	32.5	9.6	28.5	14.4	31.9	11.0	30.4
Res. Dust[a]	3.60 ± 0.57	17.1 ± 1.44	2.50 ± 0.47	14.4 ± 1.30	3.39 ± 0.29	10.3 ± 1.36	2.50 ± 0.29	10.5 ± 1.39
Brake_C[b]	1.44 ± 0.96	2.10 ± 1.26	1.21 ± 0.90	1.76 ± 1.29	0.40 ± 0.22	1.23 ± 1.17	0.34 ± 0.19	0.93 ± 1.10
Brake_D[b]	0.54 ± 0.36	1.18 ± 0.61	0.34 ± 0.31	0.68 ± 0.55	0.74 ± 0.34	1.81 ± 1.39	0.55 ± 0.33	1.97 ± 1.63
Tire Wear	1.28 ± 0.73	2.01 ± 1.10	1.21 ± 0.70	1.60 ± 0.99	1.05 ± 0.42	1.84 ± 1.56	0.96 ± 0.42	1.25 ± 1.53
Gasoline	0.77 ± 0.47	0.65 ± 0.41	0.61 ± 0.36	0.62 ± 0.36	0.26 ± 0.13	0.73 ± 0.72	0.31 ± 0.15	0.47 ± 0.46
Diesel	1.34 ± 0.68	1.48 ± 0.85	1.40 ± 0.64	1.13 ± 0.78	1.84 ± 0.45	1.92 ± 1.32	1.75 ± 0.45	1.80 ± 1.26
S. Nitrate	0.99 ± 0.11	2.34 ± 0.16	0.92 ± 0.11	2.18 ± 0.17	2.56 ± 0.21	4.81 ± 0.46	2.51 ± 0.22	3.13 ± 0.37
S. Sulfate	0.69 ± 0.19	1.28 ± 0.27	0.65 ± 0.18	1.28 ± 0.26	0.78 ± 0.12	1.16 ± 0.38	0.74 ± 0.13	1.13 ± 0.37
Others	0.23 ± 1.88	4.37 ± 3.11	0.72 ± 1.74	4.83 ± 2.88	3.33 ± 1.43	8.08 ± 3.74	1.34 ± 1.52	9.23 ± 3.76

[a] Resuspended dust.
[b] Brake_C (low copper), Brake_D (high copper); see Table S1 for profile descriptions.

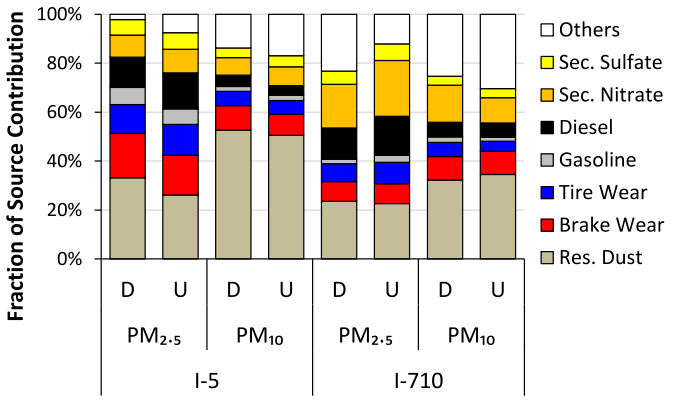

Fig. 3. Source contribution fractions at I-5 and I-710 designated downwind (D) and upwind (U) sites.

coarse PM than in fine PM. The fraction of unaccounted mass increased to 14–17% of PM_{10}.

Dust fractions were lower for the I-710 locations (22–24% for $PM_{2.5}$ and 32–34% for PM_{10}, respectively), while the fractions of secondary nitrate and unaccounted mass were higher (Fig. 3). A few elevated PM events occurring 0600–1000 LST also exhibited substantial unaccounted mass up to ~40% (Figure S2). Water-soluble ions dominated $PM_{2.5}$ and PM_{10} in these events (Wang et al., 2023) whereas water associated with the inorganic salts along with SOA could partly explain the unaccounted mass (Chen et al., 2003).

For $PM_{2.5}$, the brake and tire fractions (brake + tire = 15–17%) were comparable with the exhaust fractions (diesel + gasoline = 15–19%) at I-710. For PM_{10}, the brake and tire fractions (brake + tire) were ~14–16%, about twice the exhaust fractions (diesel + gasoline) of ~8%. These findings corroborate the CARB emission inventory, which highlights the importance of brake and tire wear. The similar breakdowns between upwind and downwind sites suggest a similar impact of on-road traffic emissions on the downwind and upwind sites.

The brake wear fraction was found to be higher than the tire wear fraction for I-5 $PM_{2.5}$, while they were comparable in I-710 $PM_{2.5}$. Oroumiyeh and Zhu (2021) found that brake and tire wear emissions increased with vehicle mass, but magnitudes of the increase were sensitive to vehicle deceleration. The generally lower traffic speeds near I-710 might explain the lower brake/tire wear ratio. Brake wear became more dominant over tire wear in PM_{10} at the I-5 and I-710 sites, though large uncertainties in the mean SCEs (Table 1) should not be overlooked.

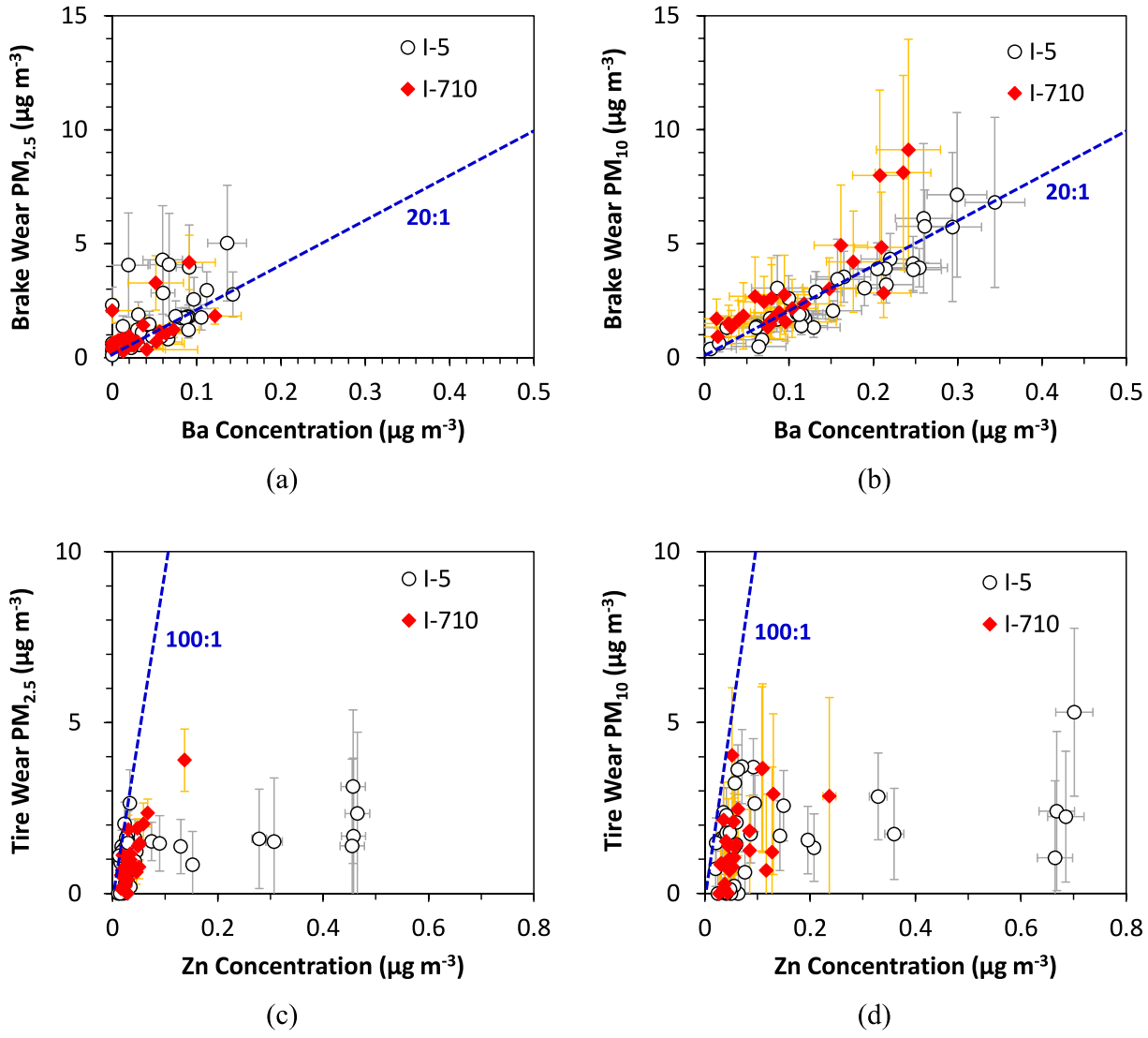

Fig. 4. Brake and tire wear contributions to $PM_{2.5}$ and PM_{10}, as quantified by EV-CMB, versus brake wear (Ba) and tire wear (Zn) markers for the I-5 and I-710 monitoring sites.

Substantial brake and tire wear particles may exist above the PM_{10} size range, which were not quantified in this study.

3.4. Variations of brake & tire wear markers and contributions

Barium is considered as a specific marker for brake wear as it is predominantly derived from brake wear in urban atmospheres (Gietl et al., 2010; Jeong et al., 2019). Jeong et al. (2019) determined a Ba mass fraction of 8.2–9.1% in brake wear related $PM_{2.5}$ in North America, which is consistent with the Ba mass fraction of 6.6–7.8% for the two brake wear profiles used in this study. A lower faction of ~1% was reported by Gietl et al. (2010) for Europe. Variations of brake PM_{10} at both I-5 and I-710 were found predictable with the measured Ba concentrations, ranging from 0.01 to 0.34 μg m^{-3}, and a scaling factor of 20 (Fig. 4 (a-b)). The highest Ba levels occurred during 0600–1000 LST on weekdays, consistent with the morning rush hours. Brake $PM_{2.5}$ contributions were not associated with Ba as well as brake PM_{10}, partly due to lower Ba concentrations (0–0.14 μg m^{-3}) and signal-to-noise ratios. A few outliers in Fig. 4 indicate possible overestimates of brake wear contributions to $PM_{2.5}$, particularly for I-5.

While tire wear markers such as benzothiazole and rubber derivatives were quantified in this study, including them in the model inputs generally lowered the goodness-of-fit and did not change the SCEs significantly. Zinc, commonly used as a tire wear marker, lacks specificity as it may also originate from brake wear and tailpipe exhausts (Panko et al., 2018). The Zn fraction of ~1% in the tire wear profile used in this study is more consistent with those in tire tread particles (0.9%) than in tire wear particles (0.3%) (Panko et al., 2018), possibly owing to differences between laboratory and real-world road surfaces. There was not a clear association between the tire PM_{10} and Zn at either I-5 or I-710. The upper edge of the tire PM_{10}-Zn scatter (100:1) in Fig. 4 is consistent with the Zn fraction in the tire wear profile, and it estimates the amount of Zn attributable to tire wear (0–0.06 μg m^{-3}). Similar scatter was found for tire wear $PM_{2.5}$-Zn with 0–0.04 μg m^{-3} Zn attributable to tire wear.

Most of the Zn observed at the monitoring sites appears to result from non-tire sources. The highest Zn concentrations (up to 0.7 μg m^{-3}) were observed at downwind and upwind I-5, in both $PM_{2.5}$ and PM_{10}, during 0600–1000 LST. These extreme Zn levels could not be explained by NTP and exhaust sources. They might inflate the SCEs for brake and tire wear and warrant further investigation. Nonetheless, this finding indicates limitations for the utilization of Zn as a sole marker for tire wear emissions.

4. Conclusion

This paper documents EV-CMB-based source apportionment for $PM_{2.5}$ and PM_{10} samples collected at near-road sites downwind and upwind of I-5 and I-710 in Los Angeles. Dust, brake wear, and tire wear source profiles were developed specifically for contemporary southern California. Sensitivity tests used the downwind-upwind differences in PM chemical composition caused by on-road traffic emissions. The optimal model revealed contributions of resuspended dust, brake wear, tire wear, and vehicle exhausts (diesel and gasoline), as well as secondary ammonium sulfate and ammonium nitrate, explaining on average 95% and 82% of $PM_{2.5}$ and 85% and 72% of PM_{10} for I-5 and I-710, respectively. Two different brake wear profiles were needed to explain the ambient measurements, one with high Cu and the other with low Cu fractions, highlighting variability of brake PM compositions.

The source contribution estimates corroborate the importance of NTP in near-road environments. Resuspended dust was found to dominate in all samples. Contributions of brake and tire wear to $PM_{2.5}$ exceeded those of tailpipe exhausts at the I-5 sites (29–30% vs. 19–21%) while they were comparable at the I-710 sites (15–17% vs. 15–19%). For PM_{10}, brake and tire wear accounted for 2–3 times the exhaust contributions. A higher fraction of HDV might explain the higher diesel (over gasoline) exhaust and high-Cu (over low-Cu) brake wear contributions near I-710, and vice versa near I-5. Only primary PM contributions were quantified in this study, though volatile organic compounds from both tailpipe and non-tailpipe (e.g., tire vapor) emissions might lead to SOA formation. The more unaccounted PM mass in I-710 samples could be attributed to SOA, sea salts, and water associated with ammonium nitrate that were not included in the CMB model.

The downwind-upwind differences of NTP and exhaust contributions were small and often insignificant, likely due to minor and nearly equal impacts from I-5/I-710 traffic on the downwind and upwind sites. This poses challenges to quantifying vehicle emission factors based on the near-road measurements. Barium can serve as a robust marker for brake wear PM, as evidenced by its strong association with brake wear contributions. On the other hand, caution should be taken to use zinc as a tire wear marker as only a small fraction of zinc appeared to result from tire wear emissions.

Author contribution

L.-W. Antony Chen: Conceptualization; Methodology; Data curation; Formal analysis; Funding acquisition; Investigation; Writing - original draft. Xiaoliang Wang: Conceptualization; Data curation; Funding acquisition; Investigation; Writing - review & editing. Brenda Lopez: Data curation; Investigation; Writing - review & editing. Guoyuan Wu: Data curation; Investigation. Steven Sai Hang Ho: Data curation; Investigation. Judith C. Chow: Conceptualization; Resources; Writing - review & editing. John G. Watson: Conceptualization; Validation; Writing - review & editing. Qi Yao: Project administration; Resources; Writing - review & editing. Seungju Yoon: Project administration; Resources; Supervision; Writing - review & editing. Heejung Jung: Funding acquisition; Investigation; Methodology; Project administration; Resources; Supervision; Writing - review & editing.

Declaration of competing interest

The authors declare the following financial interests/personal relationships which may be considered as potential competing interests: Lung-Wen Antony Chen reports financial support was provided by California Air Resources Board. Xiaoliang Wang reports financial support was provided by California Air Resources Board. Brenda Lopez reports financial support was provided by California Air Resources Board. Guoyuan Wu reports financial support was provided by California Air Resources Board. Heejung Jung reports financial support was provided by California Air Resources Board. Steven S. H. Ho reports financial support was provided by California Air Resources Board. Judith Chow reports financial support was provided by California Air Resources Board. John Watson reports financial support was provided by California Air Resources Board.

Data availability

Data will be made available on request.

Acknowledgements

This study was supported by the California Air Resources Board (CARB 18RD017). The authors thank DRI and UC Riverside staff and students, including Steve Gronstal, Steve Kohl, Chas Frederickson, David Mendez-Jimenez, Tianyi Ma, and Ling Cobb for participating in the field measurement and/or laboratory analysis, as well as Dr. Guenter Engling, Sonya Collier, Chris Ruehl, and Oliver Chang from CARB for providing technical and logistical support.

Appendix A. Supplementary data

Supplementary data related to this article can be found at https

://doi.org/10.1016/j.envpol.2023.122283.

References

Aatmeeyata, Sharma, M., 2010. Contribution of traffic-generated nonexhaust PAHs, elemental carbon, and organic carbon emission to air and urban runoff pollution. J. Environ. Eng. 136 (12), 1447–1450. https://doi.org/10.1061/(asce)ee.1943-7870.0000274.

Agudelo, C., Vedula, R.T., Collier, S., Stanard, A., 2020. Brake particulate matter emissions measurements for six light-duty vehicles using inertia dynamometer testing. SAE Int. J. Adv. Curr. Practices Mobility 3 (2020–01-1637), 994–1019.

Amato, F., Cassee, F.R., van der Gon, H.A.D., Gehrig, R., Gustafsson, M., Hafner, W., Harrison, R.M., Jozwicka, M., Kelly, F.J., Moreno, T., 2014. Urban air quality: the challenge of traffic non-exhaust emissions. J. Hazard Mater. 275, 31–36.

Amato, F., Pandolfi, M., Moreno, T., Furger, M., Pey, J., Alastuey, A., Bukowiecki, N., Prevot, A.S.H., Baltensperger, U., Querol, X., 2011. Sources and variability of inhalable road dust particles in three European cities. Atmos. Environ. 45 (37), 6777–6787. https://doi.org/10.1016/j.atmosenv.2011.06.003.

Ambade, B., Sethi, S.S., Chintalacheruvu, M.R., 2023. Distribution, risk assessment, and source apportionment of polycyclic aromatic hydrocarbons (PAHs) using positive matrix factorization (PMF) in urban soils of East India. Environ. Geochem. Health 45 (2), 491–505.

Baensch-Baltruschat, B., Kocher, B., Stock, F., Reifferscheid, G., 2020. Tyre and road wear particles (TRWP)-A review of generation, properties, emissions, human health risk, ecotoxicity, and fate in the environment. Sci. Total Environ. 733, 137823.

Beddows, D.C.S., Harrison, R.M., 2021. PM_{10} and $PM_{2.5}$ emission factors for non-exhaust particles from road vehicles: dependence upon vehicle mass and implications for battery electric vehicles. Atmos. Environ. 244, 117886 https://doi.org/10.1016/j.atmosenv.2020.117886.

Brandt, S., Perez, L., Künzli, N., Lurmann, F., Wilson, J., Pastor, M., McConnell, R., 2014. Cost of near-roadway and regional air pollution–attributable childhood asthma in Los Angeles County. J. Allergy Clin. Immunol. 134 (5), 1028–1035. https://doi.org/10.1016/j.jaci.2014.09.029.

Brugge, D., Durant, J.L., Rioux, C., 2007. Near-highway pollutants in motor vehicle exhaust: a review of epidemiologic evidence of cardiac and pulmonary health risks. Environ. Health 6 (1), 23. https://doi.org/10.1186/1476-069x-6-23.

California Air Resources Board, 2021. EMFAC 2021. https://arb.ca.gov/emfac/. (Accessed 22 March 2023).

Chen, L.-W.A., Cao, J., 2018. $PM_{2.5}$ source apportionment using a hybrid environmental receptor model. Environ. Sci. Technol. 52 (11), 6357–6369. https://doi.org/10.1021/acs.est.8b00131.

Chen, L.-W.A., Chow, J.C., Doddridge, B.G., Dickerson, R.R., Ryan, W.F., Mueller, P.K., 2003. Analysis of a summertim $PM_{2.5}$ and haze episode in the mid-Atlantic region. J. Air Waste Manag. Assoc. 53 (8), 946–956. https://doi.org/10.1080/10473289.2003.10466240.

Chen, L.-W.A., Chow, J.C., Wang, X., Cao, J., Mao, J., Watson, J.G., 2021. Brownness of organic aerosol over the United States: evidence for seasonal biomass burning and photobleaching effects. Environ. Sci. Technol. 55 (13), 8561–8572. https://doi.org/10.1021/acs.est.0c08706.

Chen, L.-W.A., Lowenthal, D.H., Watson, J.G., Koracin, D., Kumar, N., Knipping, E.M., Wheeler, N., Craig, K., Reid, S., 2010a. Toward effective source apportionment using positive matrix factorization: experiments with simulated $PM_{2.5}$ data. J. Air Waste Manag. Assoc. 60 (1), 43–54. https://doi.org/10.3155/1047-3289.60.1.43.

Chen, L.-W.A., Watson, J.G., Chow, J.C., Dubois, D.W., Herschberger, L., 2010b. Chemical mass balance source apportionment for combined $PM_{2.5}$ measurements from U.S. non-urban and urban long-term networks. Atmos. Environ. 44 (38), 4908–4918. https://doi.org/10.1016/j.atmosenv.2010.08.030.

Chen, L.-W.A., Watson, J.G., Chow, J.C., Green, M.C., Inouye, D., Dick, K., 2012. Wintertime particulate pollution episodes in an urban valley of the Western US: a case study. Atmos. Chem. Phys. 12 (21), 10051–10064. https://doi.org/10.5194/acp-12-10051-2012.

Chow, J.C., Watson, J.G., Ashbaugh, L.L., Magliano, K.L., 2003. Similarities and differences in PM_{10} chemical source profiles for geological dust from the San Joaquin Valley, California. Atmos. Environ. 37 (9–10), 1317–1340. https://doi.org/10.1016/S1352-2310(02)01021-X.

Chow, J.C., Watson, J.G., Bowen, J.L., Frazier, C.A., Gertler, A.W., Fung, K.K., Landis, D., Ashbaugh, L., 1993. A sampling system for reactive species in the western United States. In: Winegar, E.D., Keith, L.H. (Eds.), Sampling and Analysis of Airborne Pollutants. Lewis Publishers, Ann Arbor, MI, pp. 209–228.

Chow, J.C., Watson, J.G., Lowenthal, D.H., Chen, L.W.A., Zielinska, B., Mazzoleni, L.R., Magliano, K.L., 2007. Evaluation of organic markers for chemical mass balance source apportionment at the Fresno Supersite. Atmos. Chem. Phys. 7 (7), 1741–1754. https://doi.org/10.5194/acp-7-1741-2007.

Clark, L.P., Millet, D.B., Marshall, J.D., 2017. Changes in transportation-related air pollution exposures by race-ethnicity and socioeconomic status: outdoor nitrogen dioxide in the United States in 2000 and 2010. Environ. Health Perspect. 125 (9), 097012 https://doi.org/10.1289/ehp959.

Denier van der Gon, H.A., Gerlofs-Nijland, M.E., Gehrig, R., Gustafsson, M., Janssen, N., Harrison, R.M., Hulskotte, J., Johansson, C., Jozwicka, M., Keuken, M., 2013. The policy relevance of wear emissions from road transport, now and in the future—an international workshop report and consensus statement. J. Air Waste Manag. Assoc. 63 (2), 136–149.

Fabretti, J.F., Sauret, N., Gal, J.F., Maria, P.C., Scharer, U., 2009. Elemental characterization and source identification of $PM_{2.5}$ using Positive Matrix Factorization: the Malraux road tunnel, Nice, France. Atmos. Res. 94 (2), 320–329. https://doi.org/10.1016/j.atmosres.2009.06.010.

Fadel, M., Ledoux, F., Farhat, M., Kfoury, A., Courcot, D., Afif, C., 2021. $PM_{2.5}$ characterization of primary and secondary organic aerosols in two urban-industrial areas in the East Mediterranean. J. Environ. Sci. 101, 98–116.

Fitz, D.C., Judith, C., Zielinka, Babara, 2004. Development of a Gas and Particulate Matter Organic Speciation Profile Database. California Air Resources Board, Sacramento, CA.

Fujita, E.M., Campbell, D.E., Arnott, W.P., Chow, J.C., Zielinska, B., 2007a. Evaluations of the chemical mass balance method for determining contributions of gasoline and diesel exhaust to ambient carbonaceous aerosols. J. Air Waste Manag. Assoc. 57 (6), 721–740. https://doi.org/10.3155/1047-3289.57.6.721.

Fujita, E.M., Zielinska, B., Campbell, D.E., Arnott, W.P., Sagebiel, J.C., Mazzoleni, L., Chow, J.C., Gabele, P.A., Crews, W., Snow, R., Clark, N.N., Wayne, S.W., Lawson, D. R., 2007b. Variations in speciated emissions from spark-ignition and compression-ignition motor vehicles in California's south coast air basin. J. Air Waste Manag. Assoc. 57 (6), 705–720. https://doi.org/10.3155/1047-3289.57.6.705.

Ghosh, R., Lurmann, F., Perez, L., Penfold, B., Brandt, S., Wilson, J., Milet, M., Künzli, N., McConnell, R., 2016. Near-Roadway air pollution and coronary heart disease: burden of disease and potential impact of a greenhouse gas reduction strategy in southern California. Environ. Health Perspect. 124 (2), 193–200. https://doi.org/10.1289/ehp.1408865.

Gietl, J.K., Lawrence, R., Thorpe, A.J., Harrison, R.M., 2010. Identification of brake wear particles and derivation of a quantitative tracer for brake dust at a major road. Atmos. Environ. 44 (2), 141–146. https://doi.org/10.1016/j.atmosenv.2009.10.016.

Habre, R., Girguis, M., Urman, R., Fruin, S., Lurmann, F., Shafer, M., Gorski, P., Franklin, M., McConnell, R., Avol, E., Gilliland, F., 2021. Contribution of tailpipe and non-tailpipe traffic sources to quasi-ultrafine, fine and coarse particulate matter in southern California. J. Air Waste Manag. Assoc. 71 (2), 209–230. https://doi.org/10.1080/10962247.2020.1826366.

Harrison, R.M., Allan, J., Carruthers, D., Heal, M.R., Lewis, A.C., Marner, B., Murrells, T., Williams, A., 2021. Non-exhaust vehicle emissions of particulate matter and VOC from road traffic: a review. Atmos. Environ. 262, 118592 https://doi.org/10.1016/j.atmosenv.2021.118592.

Harrison, R.M., Jones, A.M., Gietl, J., Yin, J., Green, D.C., 2012. Estimation of the contributions of brake dust, tire wear, and resuspension to nonexhaust traffic particles derived from atmospheric measurements. Environ. Sci. Technol. 46 (12), 6523–6529. https://doi.org/10.1021/es300894r.

Hasheminassab, S., Daher, N., Ostro, B.D., Sioutas, C., 2014a. Long-term source apportionment of ambient fine particulate matter ($PM_{2.5}$) in the Los Angeles Basin: a focus on emissions reduction from vehicular sources. Environ. Pollut. 193, 54–64. https://doi.org/10.1016/j.envpol.2014.06.012.

Hasheminassab, S., Daher, N., Shafer, M.M., Schauer, J.J., Delfino, R.J., Sioutas, C., 2014b. Chemical characterization and source apportionment of indoor and outdoor fine particulatematter ($PM_{2.5}$) in retirement communities of the Los Angeles Basin. Sci. Total Environ. 490, 528–537. https://doi.org/10.1016/j.scitotenv.2014.05.044.

HEI, 2022. Systematic Review and Meta-Analysis of Selected Health Effects of Long-Term Exposure to Traffic-Related Air Pollution. Health Effects Institute, Boston, MA, USA.

Jalali Farahani, V., Altuwayjiri, A., Taghvaee, S., Sioutas, C., 2022. Tailpipe and nontailpipe emission factors and source contributions of PM_{10} on major freeways in the Los Angeles basin. Environ. Sci. Technol. 56 (11), 7029–7039. https://doi.org/10.1021/acs.est.1c06954.

Jeong, C.H., Wang, J.M., Hilker, N., Debosz, J., Sofowote, U., Su, Y.S., Noble, M., Healy, R.M., Munoz, T., Dabek-Zlotorzynska, E., Celo, V., White, L., Audette, C., Herod, D., Evans, G.J., 2019. Temporal and spatial variability of traffic-related $PM_{2.5}$ sources: comparison of exhaust and non-exhaust emissions. Atmos. Environ. 198, 55–69. https://doi.org/10.1016/j.atmosenv.2018.10.038.

Klöckner, P., Reemtsma, T., Eisentraut, P., Braun, U., Ruhl, A.S., Wagner, S., 2019. Tire and road wear particles in road environment–Quantification and assessment of particle dynamics by Zn determination after density separation. Chemosphere 222, 714–721.

Kumar, A., Ambade, B., Sankar, T.K., Sethi, S.S., Kurwadkar, S., 2020. Source identification and health risk assessment of atmospheric $PM_{2.5}$-bound polycyclic aromatic hydrocarbons in Jamshedpur, India. Sustain. Cities Soc. 52, 101801.

Lawrence, S., Sokhi, R., Ravindra, K., Mao, H.J., Prain, H.D., Bull, I.D., 2013. Source apportionment of traffic emissions of particulate matter using tunnel measurements. Atmos. Environ. 77, 548–557. https://doi.org/10.1016/j.atmosenv.2013.03.040.

Lin, Y.C., Tsai, C.J., Wu, Y.C., Zhang, R., Chi, K.H., Huang, Y.T., Lin, S.H., Hsu, S.C., 2015. Characteristics of trace metals in traffic-derived particles in Hsuehshan Tunnel, Taiwan: size distribution, potential source, and fingerprinting metal ratio. Atmos. Chem. Phys. 15 (8), 4117–4130. https://doi.org/10.5194/acp-15-4117-2015.

Lopez, B., Wang, X., Chen, L.-W.A., Ma, T., Mendez-Jimenez, D., Cobb, L.C., Frederickson, C., Fang, T., Hwang, B., Shiraiwa, M., 2023. Metal contents and size distributions of brake and tire wear particles dispersed in the near-road environment. Sci. Total Environ. 883, 163561.

Lough, G.C., Schauer, J.J., Park, J.-S., Shafer, M.M., Deminter, J.T., Weinstein, J.P., 2005. Emissions of metals associated with motor vehicle roadways. Environ. Sci. Technol. 39 (3), 826–836. https://doi.org/10.1021/es048715f.

Malm, W.C., Day, D.E., 2000. Optical properties of aerosols at Grand Canyon national park. Atmos. Environ. 34 (20), 3373–3391.

Oroumiyeh, F., Zhu, Y.F., 2021. Brake and tire particles measured from on-road vehicles: effects of vehicle mass and braking intensity. Atmos Environ-X 12, 100121.

Panko, J., Kreider, M., Unice, K., 2018. Chapter 7 - review of tire wear emissions: a review of tire emission measurement studies: identification of gaps and future needs.

In: Amato, F. (Ed.), Non-Exhaust Emissions. Academic Press, pp. 147–160. https://doi.org/10.1016/B978-0-12-811770-5.00007-8.

Pant, P., Harrison, R.M., 2013. Estimation of the contribution of road traffic emissions to particulate matter concentrations from field measurements: a review. Atmos. Environ. 77, 78–97. https://doi.org/10.1016/j.atmosenv.2013.04.028.

Rowangould, G.M., 2013. A census of the US near-roadway population: public health and environmental justice considerations. Transport Res D-Tr E 25, 59–67. https://doi.org/10.1016/j.trd.2013.08.003.

Timmers, V.R.J.H., Achten, P.A.J., 2016. Non-exhaust PM emissions from electric vehicles. Atmos. Environ. 134, 10–17. https://doi.org/10.1016/j.atmosenv.2016.03.017.

Wang, X.L., Gronstal, S., Lopez, B., Jung, H., Chen, L.W.A., Wu, G.Y., Ho, S.S.H., Chow, J. C., Watson, J.G., Yao, Q., Yoon, S., 2023. Evidence of non-tailpipe emission contributions to $PM_{2.5}$ and PM_{10} near southern California highways. Environ. Pollut. 317.

Watson, J.G., 2004. Protocol for Applying and Validating the CMB Model for $PM_{2.5}$ and VOC. U.S. Environmental Protection Agency, Research Triangle Park, NC.

Watson, J.G., Cooper, J.A., Huntzicker, J.J., 1984. The effective variance weighting for least squares calculations applied to the mass balance receptor model. Atmos. Environ. 18 (7), 1347–1355. https://doi.org/10.1016/0004-6981(84)90043-x, 1967.

Wik, A., Dave, G., 2009. Occurrence and effects of tire wear particles in the environment - a critical review and an initial risk assessment. Environ. Pollut. 157 (1), 1–11. https://doi.org/10.1016/j.envpol.2008.09.028.